Ionization due to multiple N- and M-shell excitation in penetrating collisions of 0.15–1.20-MeV Xe^+ with Xe†

R. A. Spicuzza and Q. C. Kessel
Department of Physics and The Institute of Materials Science, The University of Connecticut, Storrs, Connecticut 06268
(Received 31 March 1976)

The final charge states of 0.15- to 1.20-MeV Xe^+ ions scattered through angles from 1 to 20 deg by single collisions with Xe atoms have been measured. The data show the dependence of multiple N- and M-vacancy production upon the collision's distances of closest approach, which ranges from approximately 0.1 to 0.5 Å. The final charge states of those ions scattered to particular angles have average values which range from 1.5 to 16.0 in these collisions.

I. INTRODUCTION

The final charge states of 0.15–1.20-MeV Xe^+ ions scattered through angles from 1° to 20° by single collisions with Xe atoms have been measured. For the low-energy small-angle collisions, only the outermost shells can interact, and there is relatively little ionization. In the more violent of these collisions the distance of closest approach of the two nuclei is such that there is considerable interpenetration of the L shells surrounding the two nuclei, and ionization states as high as +20 are observed. Knowledge of the final charge states of the scattered ions provides information on the collision dynamics of the O, N, M, and L shells of Xe in such collisions. Similar measurements of ionization in the closely related I^{m+}-Xe collisions have been reported[1]; however, these data were obtained over a limited range of collision parameters, and they incorrectly suggest that a sharp increase in the observed ionization was due to L-shell excitation. The present data show this to be unlikely and provide detailed information on ionization resulting from N- and M-shell excitation in Xe^+-Xe collisions.

Similar differential measurements have been made at lower energies using lighter ions (including He, Ne, Ar, and Kr) at the University of Connecticut laboratories[2,3] and at the Ioffe Physical-Technical Institute.[4,5] Higher-energy investigations of the charge states of ions with energies as high as 1.8 MeV have been made by Pivovar and co-workers at the Khar'Kov Physical-Technical Institute.[6–8] Single collisions which result in inner-shell ionization are observed to have large inelastic energy losses, up to 30 keV for 12-MeV I^{m+}-Xe collisions,[9] and the corresponding ionization states can be as high as +27.[1] Many features of these data may be explained within the framework of the molecular-orbital model proposed by Fano and Lichten[10] and elaborated on by Lichten[11] and Barat and co-workers.[12,13] This is primarily a one-electron approximation and has been extensively reviewed and compared with data by several authors, among them Kessel and Fastrup,[14] who emphasized its application to single-collision phenomena, and Garcia and co-workers,[15] who emphasized its application to x-ray phenomena.

In order to establish that certain of the shell excitations observed could not have been due to the production of vacancies in the L shell, relative cross sections for L x-ray production as a function of incident ion energy were also measured. Even though the L shells of the colliding ions do interpenetrate in the more violent of the collisions investigated here, the x-ray measurements indicate that still smaller distances of closest approach are required in order for L-shell excitation to be significant for the single collisions under consideration here. This is also in agreement with inelastic energy-loss measurements currently nearing completion.[16]

II. EXPERIMENTAL METHOD

In the present investigation, Xe^+ ions are produced by a radio frequency ion source in the terminal of a 1-MV Van de Graaff accelerator, mass analyzed, and directed into a scattering chamber which has been described in a previous paper.[17] The isotopes ^{131}Xe and ^{132}Xe (not always resolved) pass through differentially pumped collimators and into the scattering region which contains Xe gas with all the isotopes present in their natural abundances. A second collimator, using rectangular apertures and subtending an angle of 0.3° from the scattering center in the plane of the apparatus, samples those Xe ions that are scattered through θ degrees by single collisions with Xe atoms. The charge of these scattered ions is determined by electrostatic analysis, and the number of ions having charge state m, N_m, are counted with a silicon surface barrier detector. The probability P_m of the beam scattered through the angle θ being found

to have charge state m is given by

$$P_m = N_m \Big/ \sum_m N_m \ . \tag{1}$$

At each of nine energies, from 0.15 to 1.20 MeV, the values of P_m were determined for a number of scattering angles between 1.0° and 20.0°. For each combination of incident-ion energy and scattering angle, the average charge of the scattered ions, $\bar{m}$, was also determined. The value of $\bar{m}$, determined from the corresponding values of P_m, is given by

$$\bar{m} = \sum_m m P_m \ . \tag{2}$$

The values of P_m determined this way are single-collision values. The target gas pressure is kept in the range of $(1-4)\times10^{-4}$ Torr, and the path length of the ions in the target gas is 2 cm; under these conditions, the probability for double collisions occurring is small. Details on the single-collision criteria used, the collimation and scattering geometry, and the cylindrical charge-state analyzer are given in the Appendix of Ref. 1.

III. EXPERIMENTAL RESULTS

The measured values of P_m are shown for selected data sets in Figs. 1–7. The solid curves represent freehand fits to the data points, and for clarity only representative points have been included in the drawing. The complete sets of data are available in Ref. 16(a). The symbols used for the various charge states in Figs. 1–7 are indicated in Fig. 1. The curves differ from those often measured[1-4,6-8] in that for a given energy the ionization does not necessarily increase with increasing angle. Such an anomaly is clearly shown in Figs. 1–3, where many of the curves are seen to have irregularities. Ordinarily, as the scattering angle increases, corresponding to a greater interpenetration of the electron shells, the degree of ionization also increases; but in the 0.25-MeV data, the charge state decreases and then increases again as the angle is increased from 4° to 5°. The same phenomenon is observed in all the data sets shown, except that the region of activity is observed to occur at smaller angles as the collision energy is increased. At 1.2 MeV the anomalous region occurs for scattering near 2°, while for

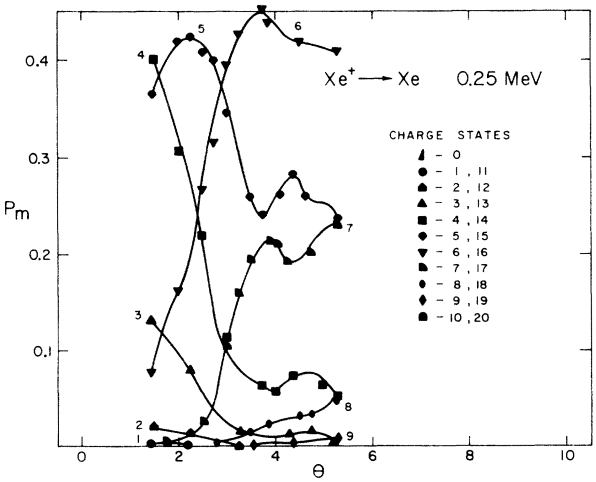

FIG. 1. Probabilities P_m for finding 0.25-MeV ions scattered through θ degrees with charge state m, plotted vs θ. For clarity it was necessary to omit some data points; thus only representative points are shown. The data scatter is of the same order of magnitude as the size of the symbols themselves. Also shown are symbols used for the various charge states in Figs. 1–7.

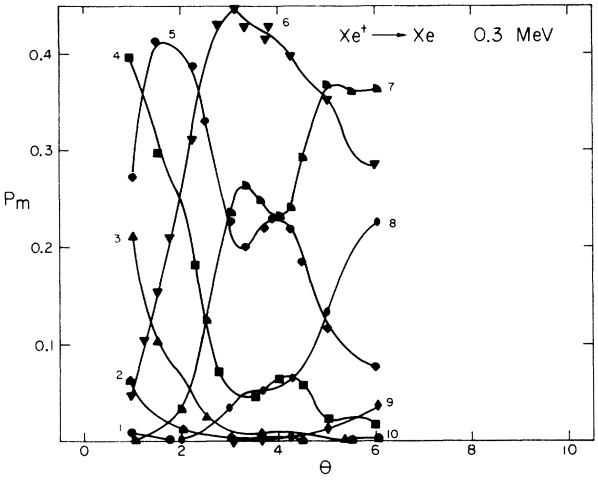

FIG. 2. Similar to Fig. 1 except for the 0.3-MeV data.

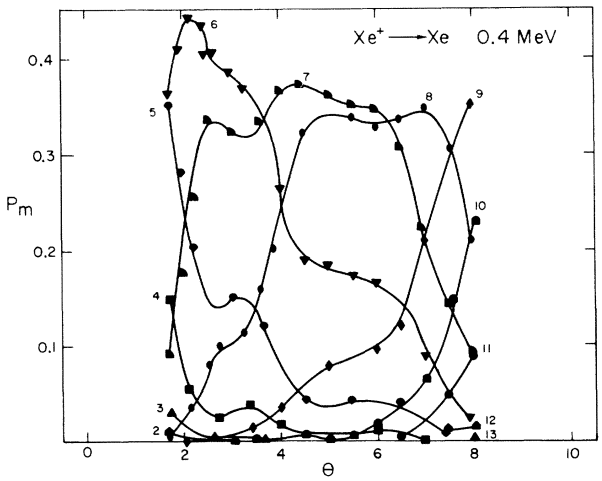

FIG. 3. Similar to Fig. 1 except for the 0.4-MeV data.

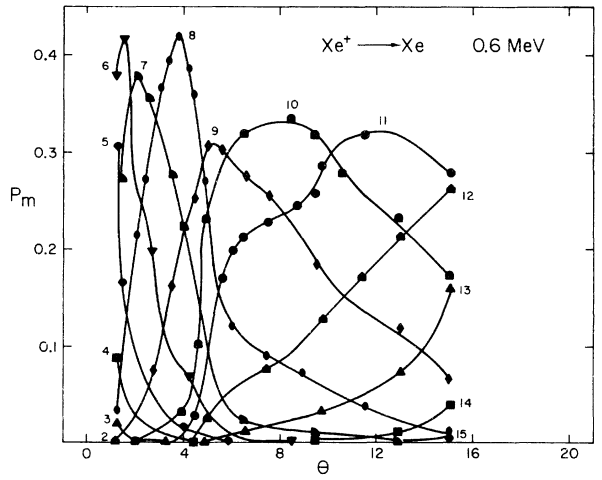

FIG. 4. Similar to Fig. 1 except for the 0.6-MeV data.

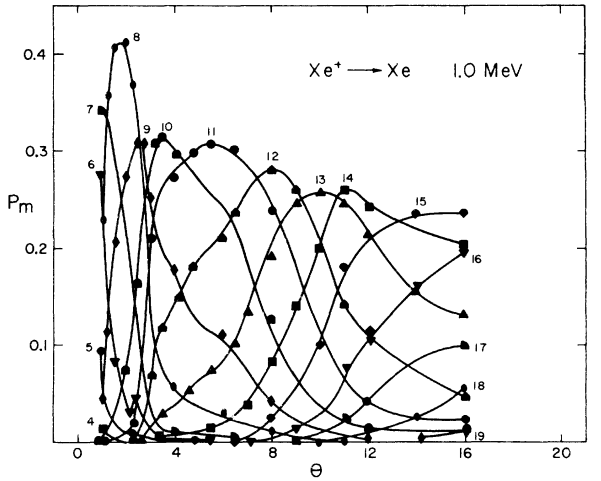

FIG. 6. Similar to Fig. 1 except for the 1.0-MeV data.

larger angles the charge-state distributions have a more usual appearance. Evidence for similar behavior in Kr^++Kr collisions is seen in the data of Ref. 5; however, evidence there for an actual decrease in ionization with increasing angle was not so strong and was not commented upon by the authors.

In Fig. 8, the average charge $\bar{m}$ is plotted versus the product $E_0\theta$ of the incident-ion energy and the scattering angle, with separate curves shown for each of several representative energies. The parameter $E_0\theta$ is useful because for small-angle scattering, the distance of closest approach R_0 is a single-valued function of $E_0\theta$.[18] Approximate values of R_0, calculated with an exponentially screened Coulomb potential,[18] are also indicated along the abscissa in Fig. 8. The value of R_0 equal to the diameter of the classical M shell of Xe, for which the M shells of two ions will begin to interpenetrate, is indicated in the figure, as is the corresponding diameter of the L shell. It is immediately evident that a wide range of collision effects give rise to the curves in Fig. 8. For the smallest values of $E_0\theta$ shown, the outer O and N shells surrounding the nuclei interpenetrate (the classical N-shell diameters are 1 Å or larger), and the average scattered charge increases by less than 0.5. In these collisions +3 is the highest ionization state observed, and we estimate that approximately 15% of the incident beam is neutralized. On the other extreme are the $E_0\theta = 24$ MeV deg data which were obtained by observing 1.2-MeV ions scattered through 20°. In these collisions, the distance of closest approach is such that the L shells of the two ions are forced to interpenetrate. Although the x-ray data discussed

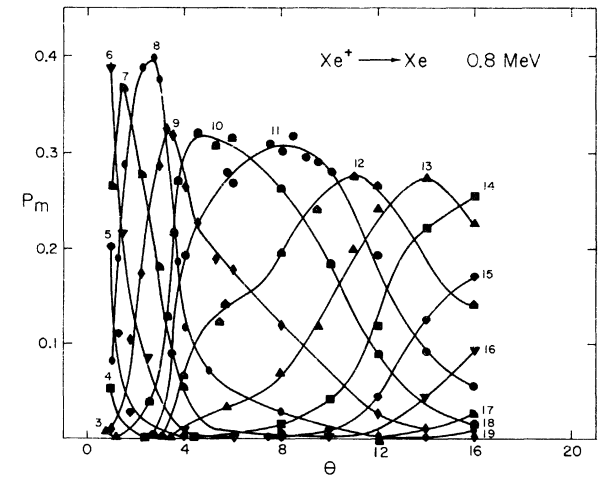

FIG. 5. Similar to Fig. 1 except for the 0.8-MeV data.

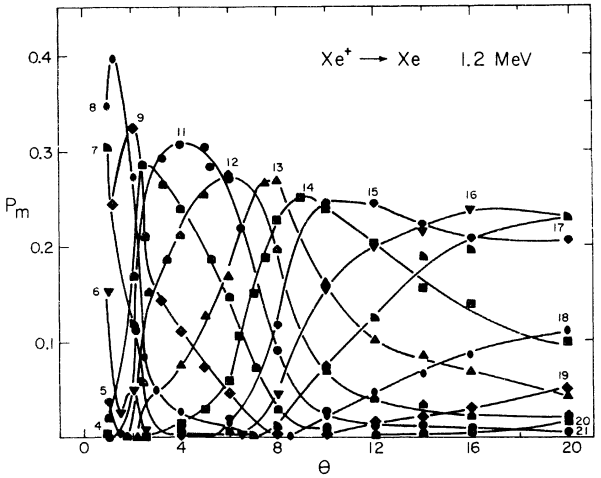

FIG. 7. Similar to Fig. 1 except for the 1.2-MeV data.

later show that no L vacancies are produced within the range of $E_0\theta$ values shown in Fig. 7, multiple vacancies are apparently produced in the N and M shells. The high-charge states which are shown in Fig. 7 and result in $\bar{m}=16$ for these collisions are presumably due to combinations of Auger-type processes occurring during the cascade filling of these vacancies.

In between these extremes, the curves exhibit several different features. As $E_0\theta$ is increased from 0.1 to 0.6 MeV deg, $\bar{m}$ increases gradually; however, at 0.6 MeV deg there is a change in slope of the curves, indicating the onset of a new excitation. The curves continue with this slope until $E_0\theta=1$ MeV deg, where $\bar{m}$ shows a decrease in its value as $E_0\theta$ increases. This is shown more clearly in Fig. 9, which is an enlargement of the first enclosed region of Fig. 8. From the break in the curve at 0.5 MeV deg to the maximum, $\bar{m}$ increases by 1. A similar increase of 1 in $\bar{m}$ follows as $E_0\theta$ increases from 1.2 to 1.6 MeV deg. At about 2.5 MeV deg, there is another abrupt rise and $\bar{m}$ increases by approximately 2. As $E_0\theta$ is increased from 8 to 20 MeV deg, $\bar{m}$ also increases, this time by about 4 to $\bar{m}=16$. The 6- and 12-MeV I^{m+}-Xe data of Ref. 1 show that out to $E_0\theta$ values of 48 MeV deg, there are no more abrupt increases in $\bar{m}$. Figure 10 shows the second enclosed region in

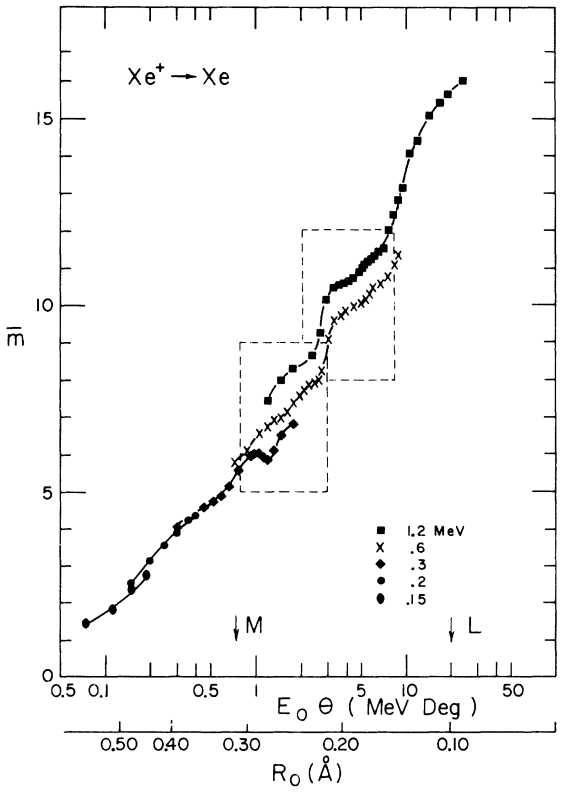

FIG. 8. Average charge $\bar{m}$ vs the product $E_0\theta$ for the data of Figs. 1–7. Separate curves are shown for each of several representative energies, and approximate values of R_0 are also shown along the abscissa. The outlined areas are shown in greater detail in Figs. 9 and 10.

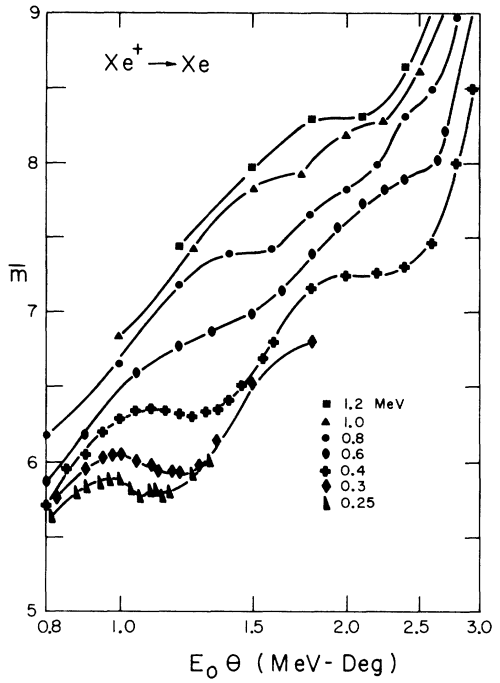

FIG. 9. Region of Fig. 8 between $E_0\theta=0.8$ and 3.0 MeV deg shown in greater detail.

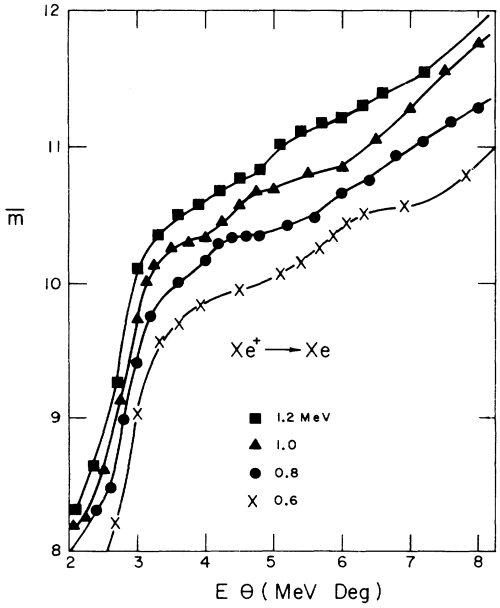

FIG. 10. Region of Fig. 8 between $E_0\theta=2.0$ and 8.0 MeV deg shown in greater detail.

Fig. 8 in greater detail. The increase in $\bar{m}$ by 2 between $E_0\theta = 2$ and 3 MeV deg is seen clearly. However, the curves show a very different nature between $E_0\theta = 3$ and 8 MeV deg. The uncertainty in the data points is equal to or less than the size of the symbols in the figure, and therefore the irregularities shown are meaningful.

The width and asymmetry of each of the charge-state distributions in Figs. 1–7 have been calculated. The distribution width or standard deviation σ of the percentages from the average charge $\bar{m}$ may be defined by

$$\sigma^2 = \sum_m (i - \bar{i})^2 P_m \ . \tag{3}$$

The asymmetry or skewness γ of such a distribution may be defined by

$$\gamma = \sum_m \frac{(i - \bar{i})^3 P_m}{\sigma^3} \ . \tag{4}$$

Figure 11 shows the approximate values of σ and γ associated with the data, plotted versus $E_0\theta$. Except for some scatter, all of the data points fall within the indicated bands. The band for σ shows a behavior almost identical to that of $\bar{m}$ when plotted versus $E_0\theta$. Plotting σ versus $\bar{m}$ shows that to a first approximation σ is a linear function of $\bar{m}$. The plot of γ vs $E_0\theta$ shows that the distributions are remarkably symmetric. Except for a variation in the very-low-energy data, γ has only a slight tendency toward negative values. A negative value of γ corresponds to an asymmetric distribution having the higher charge states bunched near $\bar{m}$ and the lower charge states tailing off less rapidly on the other side of $\bar{m}$.[19]

Reference 1 suggested that a rise in $\bar{m}$, corresponding to the present rise at $E_0\theta \cong 10$ MeV deg in Fig. 8, was due to L-shell excitation, because the corresponding value of R_0 is such that the L shells of the two ions begin to overlap in those collisions. To test the validity of this suggestion, the relative cross section for L x-ray production was measured with a proportional counter. This cross section is plotted as a function of the incident-ion energy in Fig. 12. From the threshold behavior of this curve, an approximate threshold value of R_0 below which L x rays may be produced in these collisions is easily calculated if one assumes the L-shell excitation probability to be a stepwise function of R_0.[20] This has proven to be a reasonable approximation for other cases of L-shell excitation,[14] and should at least give an approximate value for the threshold in the present

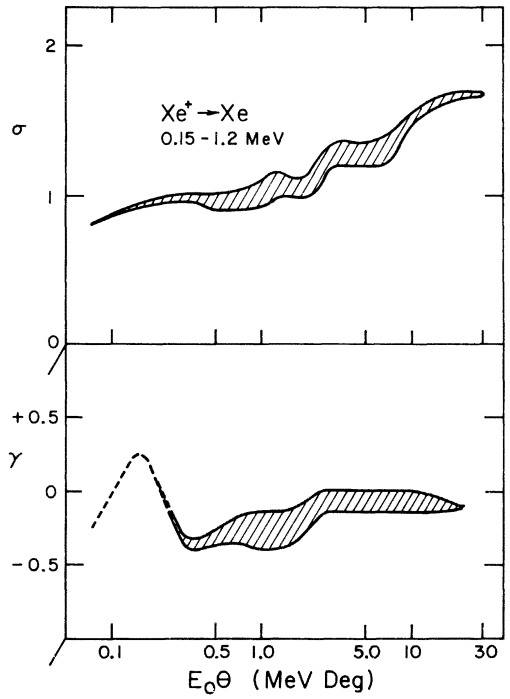

FIG. 11. Charge-state distribution widths σ and asymmetries γ vs $E_0\theta$.

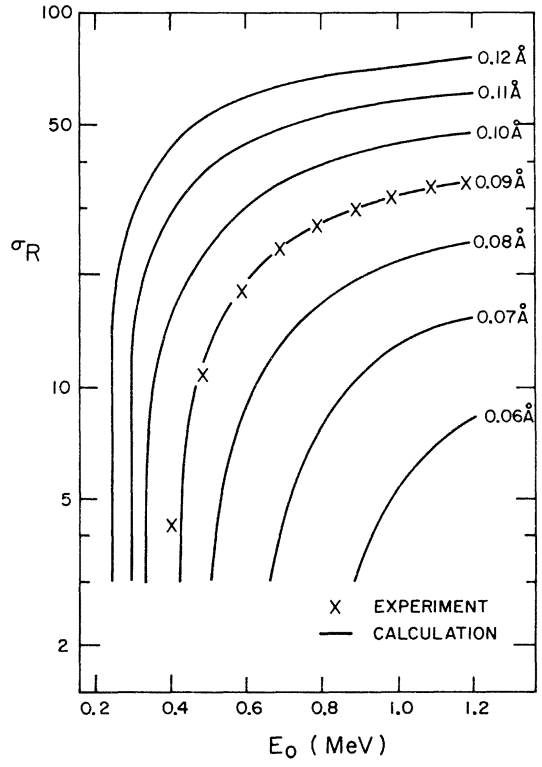

FIG. 12. Relative total cross sections for the production of Xe L x rays shown as a function of incident-ion energy. The solid curves result from a calculation in which R_0 is treated as a variable parameter.

case. The solid curves in Fig. 12 are the result of such a calculation, and the threshold value for R_0 used in the calculation of each curve is indicated. Because the increase in $\bar{m}$ in question begins at $R_0 \cong 0.12$ Å and the x-ray data show a threshold of about 0.09 Å, for L x-ray production, it is unlikely that any of the data in Fig. 8 are influenced by L-shell excitations. This conclusion is in agreement with the solid-target data (I^{m+}-Te) of Stein and co-workers[21] and preliminary inelastic energy-loss measurements for Xe^+-Xe collisions made by the present authors.[16]

IV. DISCUSSION

The explicit interpretation of these data is difficult because of the numerous interactions between the various shells which are theoretically possible. This complexity is illustrated by the partial molecular-orbital (MO) correlation diagram for the Xe-Xe molecule presented in Fig. 13. This figure is based upon a nonrelativistic one-electron approximation, and drawn according to the rules suggested by Lichten and co-workers.[11,12] Calculations of some of these levels are currently in progress,[22] and the inclusion of relativistic effects may possibly shift some of the correlations[23]; however, the present diagram will still serve as a useful basis for discussion.

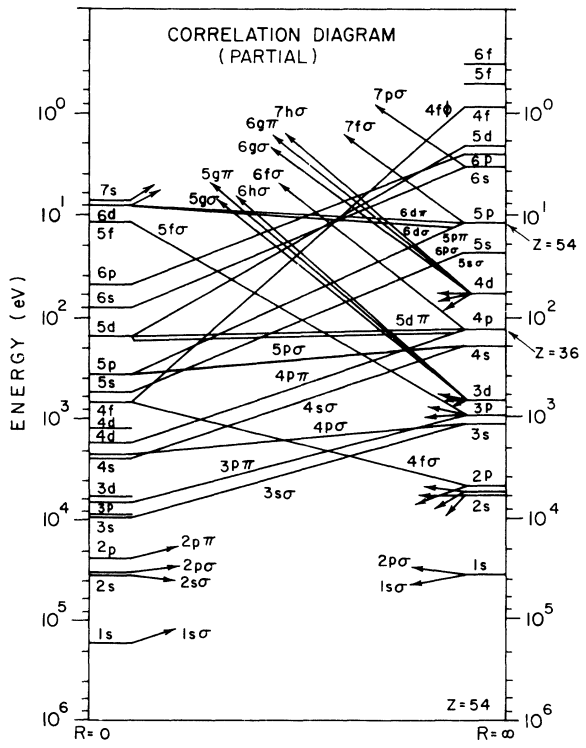

FIG. 13. Partial one-electron correlation diagram for the Xe-Xe system drawn according to the rules provided by Lichten and co-workers (Refs. 11 and 12). The levels filled for $Z=36$ (Kr) and $Z=54$ (Xe) are indicated.

A. L-shell excitation

The emission of L x rays from single collisions of Xe^+ with Xe demonstrates that a mechanism must exist for the production of L vacancies in such collisions. Of the interactions under consideration here, probably the L-shell excitations are described to the best approximation by the MO model. For other collision combinations, $2p$ electrons in the separated atoms (SA) have been observed to be promoted by the $4f\sigma$ MO to higher levels.[14] Reference to Fig. 13 shows this to be a likely possibility in the present case too. With the exception of the $4f\sigma$ orbital, all other orbitals which correlate with the SA L levels lead to closed excitation channels; i.e., all their possible crossings are with filled MO's. The $4f\sigma$ MO, on the other hand, crosses several filled levels until, in the united-atom (UA) limit, it becomes degenerate with the $4f\phi$ MO. Both of these levels correlate with the $4f$ level in the UA limit. The $4f\phi$ MO correlates with the SA $4f$ level and may contain some vacancies, because the $4f$ SA level is an unfilled level (in Xe, the $5p$ level is the last filled shell, as indicated in Fig. 13). For the SA L electrons to be promoted in this manner ($4f\sigma \rightarrow 4f\phi$), the coupling would have to be rotational in nature. In fact, the increase would have to be by three units of angular momentum along the internuclear axis. This would be a velocity-dependent excitation, which is consistent with the velocity dependence of the higher-energy $\bar{m}$ and inelastic energy-loss data of Refs. 1 and 9. The R_0 values in these higher-energy collisions correspond to a significant overlapping of the L shells of the two ions.

B. M-shell excitation

The previous discussion shows that the rise in $\bar{m}$ at $E_0\theta = 10$ MeV deg is not due to L-shell excitation, and it is therefore appropriate to assume it is due to M-shell excitation. Indeed, preliminary inelastic energy-loss measurements show that both the rise at 10 MeV deg and the rise at 3 MeV deg correspond to energy losses which average 350–600 eV per additional electron removed.[16] These energies are consistent with the Auger electron energies observed by Thomson in 200-keV Xe^+-Xe collisions. He has observed groups of electrons having energies of approximately 50, 350, and 450 eV.[24] The latter two peaks would be energetically consistent with the filling of the

SA $3d$ level with electrons from the $4s$ or $4p$ levels. The only firm conclusion that can be drawn from this information is that these collisions do create vacancies in the M shell of the Xe atoms, almost certainly in the $3d$ level. Reference to Fig. 13 shows three MO's, the $6h\sigma$, the $5g\pi$, and the $5g\sigma$, as likely channels for the promotion of $3d$ electrons. Fastrup and co-workers have observed the removal of $3d$ electrons in Kr^+-Kr collisions, and have attributed this to the promotion of these electrons along the $6h\sigma$ MO, because this is the first MO correlating with the $3d$ level to be promoted as the nuclei approach each other.[22,25] Further data obtained by Afrosimov and co-workers support this interpretation.[26] A similar situation holds here, except that many of the initial crossings are with filled orbitals in the Xe-Xe case. In consideration of the above, we attribute the rise in $\bar{m}$ at 3 MeV deg to the promotion of two $3d$ electrons (one from each atom) along the $6h\sigma$ MO. The increase in $\bar{m}$ of approximately 2 is what might be expected from the cascade filling of a single $3d$ vacancy in the scattered ion. The rise in $\bar{m}$ at $E_0\theta = 10$ MeV deg we then attribute to promotions of additional $3d$ electrons by the $5g\pi$ MO. This MO requires further interpenetration of the electron shells before being promoted. Being a π orbital it can promote up to four electrons (perhaps two from each atom), and the greater increase in $\bar{m}$ at 10 MeV deg when compared with that at 3 MeV deg is consistent with this.

Within the framework of the present interpretation, interference between outgoing channels might be possible. The irregularities in the curves of Fig. 8 are suggestive of interference effects; however, the present data do not allow the identification of specific outgoing channels for the promoted electrons. X-ray experiments by Fortner and co-workers do show evidence for one possible outgoing channel, the filling of the normally vacant $4f$ level upon separation of the nuclei.[27] Their observation of $4f \rightarrow 3d$ x rays from these collisions is evidence for transferral of some electrons, but not necessarily $3d$ electrons, into the $4f\phi$ MO.

C. N-shell excitation

The onset of N-shell excitation occurs at approximately $E_0\theta = 0.6$ MeV deg, and is the dominant feature in the curves of Figs. 8 and 9 until $E_0\theta$ exceeds 2.5 MeV deg and M-shell excitations predominate. As before, it is on the basis of preliminary inelastic energy-loss measurements that we attribute these excitations to N-shell interactions; the ionizations correspond to energy losses which average 50–100 eV per additional electron removed.[16]

The curves in Fig. 9 display a double rise with a pronounced energy dependence. This double rise, with each rise corresponding to approximately one additional ionization, is most clearly seen in the 0.4-MeV data. After an increase in $\bar{m}$ of 1 between $E_0\theta = 0.6$ and 1.0 MeV deg, there is no further ionization until 1.4 MeV deg, at which point $\bar{m}$ increases by unity once again. As the collision velocity is increased, the $E_0\theta$ values for which the increases in $\bar{m}$ occur also move toward higher values of $E_0\theta$. This is opposite to the trend usually shown by this type of data,[14] where thresholds tend to occur at lower values of $E_0\theta$ when the collision velocity is increased. The actual decrease in ionization which occurs between these excitations is also unusual and might be due to interference effects. It is this anomaly which causes the irregularities in the curves in Figs. 1–6.

D. Higher-energy measurements

Alton and co-workers[28] and Bridwell and co-workers[29] have measured the absolute yields for the production of high-charge states by 20- and 60-MeV collisions of I^{m+} with Xe. These measurements have been made for scattering angles from 0° to 1.5°, and therefore have $E_0\theta$ values overlapping with those of the present work. However, it is difficult to compare our results with these experiments, because the ionization states of the incident projectiles are different; Ref. 28 presents results for 20-MeV I^{6+}-Xe collisions, and Ref. 29 for 60-MeV I^{10+}-Xe collisions. Reference 28 reports also on the variation of the scattered-charge states as a function of target-gas pressure. The pressures used range from those which result in multiple-collision charge equilibrium down to pressures which approximate the single-collision conditions used in the present experiment. Where comparisons can be made the results are consistant, suggesting that at least the gross features of the higher-energy data have the same origin as the structure in the present data. An important feature of the data in Refs. 28 and 29 is that they are absolute measurements and demonstrate the feasibility of producing experimentally useful beams of the highly charged ions described here.

ACKNOWLEDGMENTS

The authors have profited from discussions with many individuals. Among those to whom we are indebted are Jörg Eichler, Joseph Macek, Arnold Russek, George Thomson, and Uwe Wille.

†Research supported by the National Science Foundation.

[1]Q. C. Kessel, Phys. Rev. A 2, 1881 (1970).
[2]E. N. Fuls, P. R. Jones, F. P. Ziemba, and E. Everhart, Phys. Rev. 107, 704 (1957).
[3]E. P. Ziemba, G. J. Lockwood, G. H. Morgan, and E. Everhart, Phys. Rev. 118, 1552 (1960).
[4]D. M. Kaminker and N. V. Fedorenko, Zh. Tekh. Fiz. 25, 2239 (1955).
[5]V. V. Afrosimov, Yu. S. Gordeev, M. N. Panov, and N. V. Fedorenko, Zh. Tekh. Fiz. 36, 123 (1966) [Sov. Phys.-Tech. Phys. 11, 89 (1966)].
[6]L. I. Pivovar, M. T. Novikov, and V. M. Tubaev, Zh. Eksp. Teor. Fiz. 46, 471 (1964) [Sov. Phys.-JETP 19, 318 (1964)].
[7]L. I. Pivovar, M. T. Novikov, and A. S. Dolgov, Zh. Eksp. Teor. Fiz. 50, 537 (1966) [Sov. Phys.-JETP 23, 357 (1966)].
[8]L. I. Pivovar, G. A. Krivonosov, and V. M. Tubaev, Zh. Eksp. Teor. Fiz. 53, 1872 (1967) [Sov. Phys.-JETP 26, 1066 (1968)].
[9]Q. C. Kessel, P. H. Rose, and L. Grodzins, Phys. Rev. Lett. 22, 1031 (1969).
[10]U. Fano and W. Lichten, Phys. Rev. Lett. 14, 627 (1965).
[11]W. Lichten, Phys. Rev. 164, 131 (1967).
[12]M. Barat and W. Lichten, Phys. Rev. A 6, 211 (1972).
[13]J. C. Brenot, D. Dhuicq, J. P. Gauyacq, J. Pommier, V. Sidis, M. Barat, and E. Pollack, Phys. Rev. A 11, 1245 (1975).
[14]Q. C. Kessel and B. Fastrup, Case Stud. At. Phys. 3, 137 (1973).
[15]J. D. Garcia, R. J. Fortner, and T. M. Kavanagh, Rev. Mod. Phys. 45, 111 (1973).
[16](a) R. A. Spicuzza, Ph.D. thesis (University of Connecticut, 1976) (unpublished). (b) See also Q. C. Kessel and R. A. Spicuzza, in *Abstracts of Papers of the Ninth International Conference on the Physics of Electronic and Atomic Collisions*, edited by J. S. Risley and R. Geballe (Univ. of Washington Press, Seattle, 1975), Vol. 2, p. 1171; R. A. Spicuzza, A. A. Antar, and Q. C. Kessel (unpublished).
[17]Q. C. Kessel, Rev. Sci. Instrum. 40, 68 (1969). The authors are grateful to High Voltage Engineering Corporation, Burlington, Mass., for making the chamber available for this investigation.
[18]E. Everhart, G. Stone, and R. J. Carbone, Phys. Rev. 99, 1287 (1955). This classical calculation makes use of a screened Coulomb potential. [See also F. W. Bingham, J. Chem. Phys. 46, 2003 (1967).] Extensive tables of this and other classical collision parameters have been prepared by Felton W. Bingham and are available as Document No. SC-RR-66-506, *Tabulation of Atomic Scattering Parameters Calculated Classically from a Screened Coulomb Potential* (Clearinghouse for Federal Scientific and Technical Information, U. S. Nat. Bur. Stand., Springfield, Va.), (price $3.00).
[19]Equations (3) and (4) in Ref. 1 are incorrect in that $\bar{i}-i$ should read $i-\bar{i}$.
[20]Q. C. Kessel, Bull. Am. Phys. Soc. 14, 946 (1969).
[21]H. J. Stein, H. O. Lutz, P. H. Mokler, and P. Armbruster, Phys. Rev. A 5, 2126 (1972).
[22]J. Eichler and U. Wille (private communication). See also J. Eichler and U. Wille, Phys. Rev. A 11, 1973 (1975).
[23]B. Fricke (private communication). See also B. Fricke, K. Rashid, P. Bertoncini, and A. C. Wahl, Phys. Rev. Lett. 34, 243 (1975).
[24]George Thomson (private communication). See also L. O. Werme, T. Bergmark, and K. Siegbahn, Phys. Scr. 6, 141 (1962), for the *M-NN* Auger spectra of electron excited Xe.
[25]B. Fastrup and G. Hermann, Phys. Rev. A 3, 1955 (1971).
[26]V. V. Afrosimov, Yu. S. Gordeev, A. M. Polyanski, and A. P. Shergin, in *Proceedings of the Seventh International Conference on the Physics of Electronic and Atomic Collisions, Amsterdam, 1971, Abstracts of Papers*, edited by L. M. Branscomb *et al.* (North-Holland, Amsterdam, 1972), p. 397; V. V. Afrosimov, in *Proceedings of the International Conference on Inner Shell Ionization Phenomena and Future Applications, Atlanta, 1972*, edited by R. W. Fink *et al.*, CONF-720404 (Natl. Tech. Information Service, U.S. Dept. of Commerce, Springfield, Va. 22151), p. 1297.
[27]R. J. Fortner, R. C. Der, and T. M. Kavanagh, Phys. Lett. 37A, 259 (1971).
[28]G. D. Alton, J. A. Biggerstaff, L. B. Bridwell, C. M. Jones, Q. Kessel, P. D. Miller, C. D. Moak, and B. W. Wehring, IEEE Trans. Nucl. Sci. NS-22, 1685 (1975).
[29]L. B. Bridwell, J. A. Biggerstaff, G. D. Alton, C. M. Jones, P. D. Miller, Q. Kessel, and B. Wehring, in *Proceedings of the Fourth International Conference on Beam-Foil Spectroscopy and Heavy-Ion Atomic Physics, Gatlinburg, Tenn., 1975* (Plenum, New York, 1976), p. 657-664.